World Journal of Pharmaceutical and Life Sciences
WJPLS
www.wjpls.org
SJIF Impact Factor: 6.129

PHOTOCATALYTIC DEGRADATION ACTIVITY OF AROMATIC COMPOUND BY TIO2 NANOPARTICLES

Farah S. Daabool*

College of Biotechnology, Al-Qasim Green University, Hilla, Iraq.

Corresponding Author: Farah S. Daabool
College of Biotechnology, Al-Qasim Green University, Hilla, Iraq.

Article Received on 21/01/2022 **Article Revised on 11/02/2022** **Article Accepted on 01/03/2022**

ABSTRACT

TiO2's capacity as a photocatalyst and its great performance in photovoltaic applications have been the subject of extensive research .In this study, TiO2 nanoparticles were examined for phenol degradation under UV radiation in a range of pH conditions.SEM and XRD were employed to describe the TiO2 nanoparticle. The outcomes demonstrated that Titanium dioxide nanoparticles have an anatase-like structure and a 26 nm particle size. Breakdown of phenol by UV light had phenol remove of 77% phenol was destroyed in 2 hours, whereas the degradation of phenol without UV rays had removal efficiency of 15% dye was destroyed in 2 hrs, according to the efficiency of photocatalysis of TiO2 nanoparticle. It said that UV light could trigger the efficiency of photocatalysis of Titanium dioxide nanoparticles. The breakdown of phenol 15% is no a photocatalysts activity; rather, it is the destruction of phenol by Titanium dioxide nanoparticles without the availability of UV light. Titanium dioxide nanoparticles' photocatalytic activity is pH-sensitive. Titanium dioxide nanoparticles have the efficiency of photocatalysis of 77% in neutral conditions (pH 7.0), the highest photocatalytic activity occurs.

KEYWORD: TiO2, photo degradation phenol, XRD, SEM.

1. INTRODUCTION

The titanium dioxide's and's photocatalytic capabilities and their great effectiveness in photovoltaic applications have been extensively explored.[1-5] Because of its high Activity, TiO2 has recently generated a lot of interest in the field of environmental cleaning.[6] Additionally, it demonstrates chemical stability, few toxicity, few pollutant load, and low cost.[7] To enhance the reactivity surface area and boost efficiency, Titania size has been decreased.[8] Numerous organic contaminants can be successfully degraded by TiO2 photocatalytic wastewater treatment, according to research.[9]

TiO2 has been employed as a photocatalyst extensively because of its high stability and economic availability . TiO 2 has been synthesized in a variety of forms, including nanoparticle, nanotube, nanofiber, and nanosheet.[10] The utilization of Titanium dioxide in the wastewater treatment process is the subject of numerous initiatives.[11] The pH of a solution is a crucial factor in the photocatalysts reactions occurring on particle surfaces due to it controls the surface tension characteristics of the photocatalyst as well as the aggregate sizes it generates.[12] Due to the attained severe circumstances, the dissociation of oxygen and water molecules is a process that is frequently see.[13] The pH may have a significant impact on how well drugs are removed from the environment.Regarding photolysis, different species may have different transformation products, rates of mechanism-based degradation, and photolytic degradation routes.[14] The facts that the structure orientation of the molecules favors the assault of the oxidation products under all those conditions may possibly be a contributing factor to the higher breakdown rate in acidic or basic pH.

The rate of deterioration for the breakdown and While the rate of the pesticide's degradation and mineralization was shown to decrease with an increase in pH solution, degradation of acid red was shown to rise with an increase in pH solution.[15] Due to its many functions, including electrostatic attractions between the surface of the semiconductor, charged radicals, solvent molecules, and the substrate produced throughout the reaction, interpreting pH impacts on the photocatalytic activity is a particularly challenging endeavor. There have been many tries, but no satisfactory justification.

We will talk about how a substance's pH is pollutant phenol effect of the solution photoactivity of TiO2 nanoparticles in this study. It has been proposed that ZnO nanoparticles, which have a higher exciton binding energy than TiO2 nanoparticles and are used in a variety of catalysts including responsive electronic goods,

ultraviolet (UV) light emitters, chemical sensors, spin electronics, and piezoelectric devices, are more promising UV emitting phosphors because of their unique properties and wide range of applications (60 meV). This characteristic lowers the UV lasing thresholds and results in greater UV.[16] At ambient temperature, emission effectivenessThe potential exists to increase the efficiency of photocatalysis processes because of the increased surface area of nanosize Zinc Oxide compared to bigger particles.

According to a paper, smaller TiO2 and ZnO particles have a higher redox potential because of the photocatalytic breakdown of organic toxins when exposed to UV rays. The created TiO2 and Zinc oxide nanoparticles can be viewed as the optimal photocatalysts for industrial-scale environmental cleaning in a central pH environment.[17] Numerous researchers have looked into the photocatalytic destruction of inorganic and organic contaminants on various semiconductor types. indirect response at the holes that are positive, which form in the valence band semiconductor after that migrate to surface of catalyst and participate in inter - facial oxidation-reduction reactions, is thought to be the cause of Adsorbed colored materials oxidize in the valence band between the valence band. either organic or inorganic molecules. However, in the nanoparticles dispersed, the band gap was reduced, which decreased the recombination process.[18] In the past, the Langmuir-Hinshelwood rates model and the pseudo first order reactive kinetic model have been used to explain the photocatalytic color removal process.[19] This investigation looks at the sol-gel process for producing titanium dioxide, explores effects on particle sizes, and contrasts the photocatalytic activety of the generated nanoparticles that of the base material.

2. Experimental

2.1. Materials and methods

We bought TiCl 4 (99.99%) from the Flucka Company.

%99.98) purity is guaranteed for absolute ethanol, according to the Gainland Chemical Company (GCC.(phenol is a pollutant (supplied from Fluka company.(TiO2 nanoparticles were generated under normal environmental conditions.

2.2. Preparation of phenol solution

Prepare standard solution of phenol is deferent concentration 10,20,40,60 and 80 ppm to calibration curve and choose 60 ppm in 1 liters for degradation by take 60 mg in 1000 ml .

2.3 TiO2 nanoparticle preparation

An earlier methodology that was modified was used to create the TiO2 nanoparticles.[20]

The following was the method's explanation:

10ml of TiCl4 and 100 milliliters of pure ethanol were introduced drop - wise to a reaction mixture because the reaction is exothermic, TiCl4 is very volatile, and it produces hydrogen chloride as fast as it is added.

Following 15 hours of dried at 85°C inside an oven, the resultant solution went from clear to yellow and formed TiO2 nanopowder as in figure 1.

TiO2 nanopowder was eventually formed in a variety of phases by splitting all produced powder into seven sections and heating the obtained powdered in a furnace at heats equal to 400 °C.

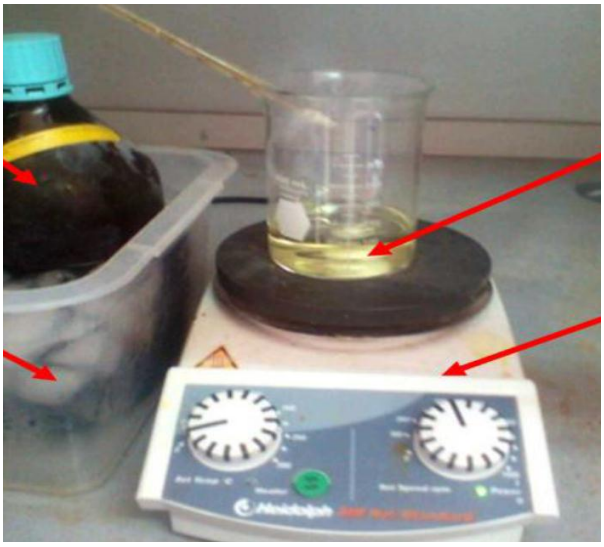

Figure 1: Summarizes this technique.

2.4. Calibration Curve

In order to create the calibration curves, standardized phenol aqueous solutions were used.

At 269 nm, the absorption of each quantity was determined.

Table 1 presents the normal calibration values, which are shown in Figure 2-3.

Table 1: Absorbance of different phenol concentrations.

Con. (ppm)	Abs. in 269 nm
0	0
10	0.19
20	0.36
30	0.55
40	0.73
50	0.91
60	1.09
70	1.24
80	1.47

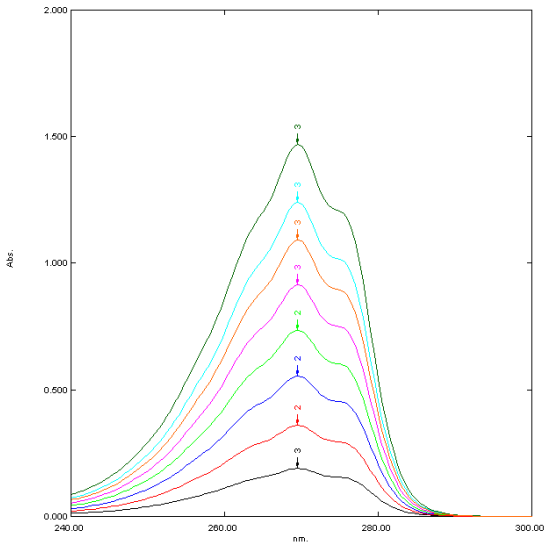

Figure 2: Shows the UV-visible spectra of phenol at various concentrations.

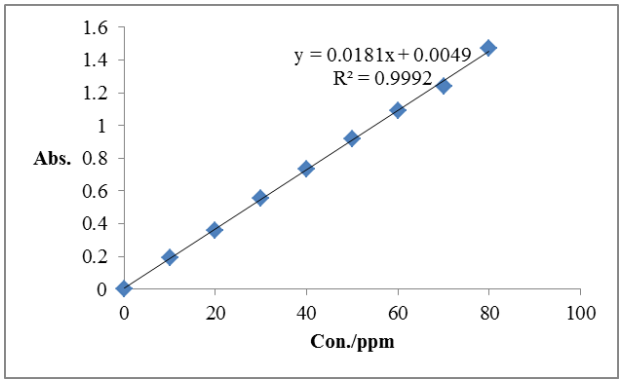

Figure 3: Calibration curve for different concentrations at 269 nm for phenol.

2.5. Characterization

A Philips X-ray diffraction pattern (PW 1730) was employed for X-ray diffraction with automatic data collection using Cu K radiation (= 0.15406 nm) and operated at 40 kV/30 mA. (APD Philips v3.6B.)

The diffract patterns mostly in 20o to 60o range were gathered using a 0.05o step length and a 2 second capture duration in step.

The diffractometer had to be calibrated before each measurement could be made.

The basis for the XRD calculation of crystallite size was the Scherrer equation.[1]

2.6. Synthetic Methods for TiO2 Nanostructures

TiO2 nanoparticles can be created using a variety of techniques.

Typically, nanoparticles, nanowires, nanowires, and nano - tubes are the main end products. Both gas and liquid techniques can be used to create nano-TiO2. Due to the need for specialized equipment, gas procedures are typically more challenging than liquid ones. Among the procedures utilized to make nano-TiO2 are hydrolysis, drying, and calcinations.

The pursuit of affordable, high-quality products has been a constant endeavour. Due to their affordability and high titanium concentration, a number of substances, including titanium tetrachloride (TiCl4)), can be employed as raw materials to produce nano-TiO2. TiCl4 has been used in a number of different ways to create nano-TiO2.[21]

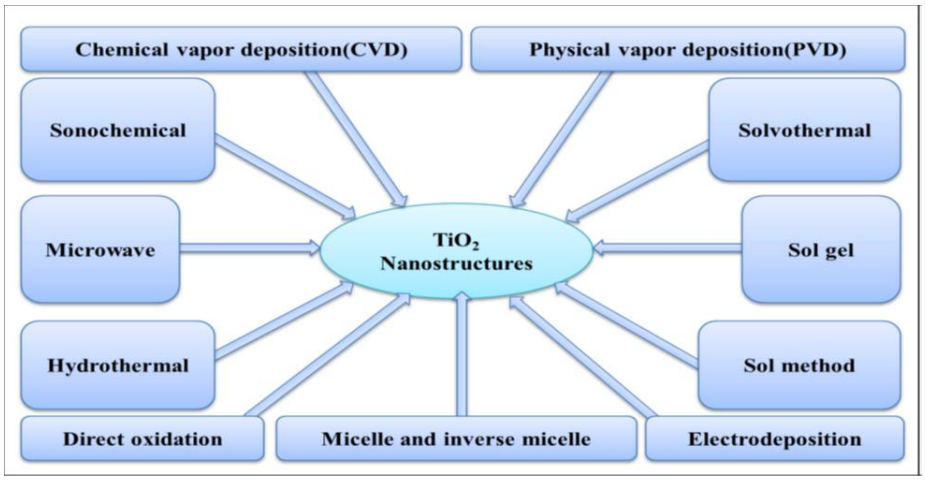

Figure 4: Methods to synthesis TiO2 nanoparticles.

2.6.1. Sol-Gel Method

Growing numbers of novel materials have been developed using the sol-gel process, including those for catalyse,[22] biosensors,[23] membrane,[24] fiber,[25] electro - optic gain surfaces,[26] photosensitive and nonlinear uses,[27] and liquid - solid electrochemical devices.[28]

TiO2 nanopowder is created using the most significant sol-gel technique.

With this technique, ultrafine powder can be produced, which has highly disproportionate surface to volume and a strong impulse to clump together. By heating, we mean the adherence of particles to one another due to the attraction of van der Waals interactions. Sintering necks form covalent bonds between these particles. As a result, these pressures are strong in the instance of nanoscale, resulting in nanopowder with a large surface area. Precursors in a typical procedure are often inorganic materials salts or organic metal compounds like metal halides.

These undergo exothermic hydrolysis and polymerization, which results in the formation of a colloidal dispersion or sol.

As illustrated in Figure 5, the solvent is completely polymerized and lost by calcination during the change from the liquid phase to solid gel phase.

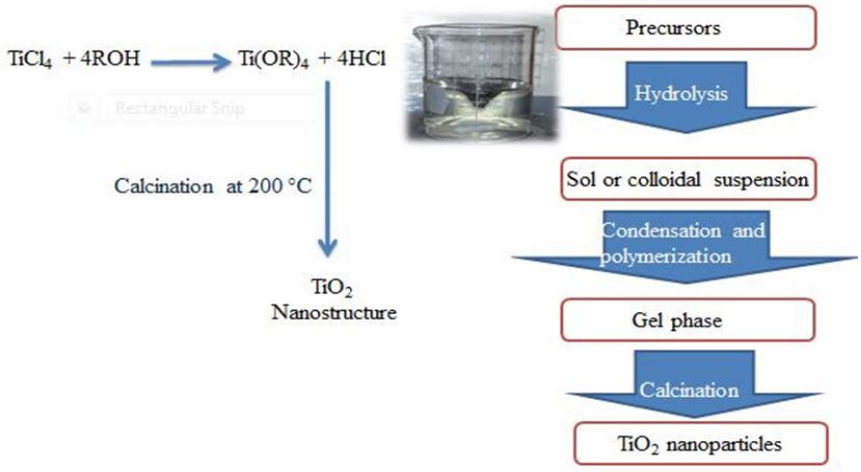

Figure 5: Procurer to synthesis TiO2 nanoparticles.

2.7. Photocatalytic Activity Experiments

To use a 100 mL photoreactor, the studies on photocatalytic activity were carried out.

The radiation utilized had a typical wavelength of = 269 nm and was produced by a Philips (CLEO, Poland) mercury lamp with four 15W bulbs that produced a 600 mW Hg lamps UV(A) at a strength of 0.7 mW/cm2. The suspended solutions were created by mixing 100 mL of a phenol aqueous solution with a 60 ppm concentration with 175 mg of nanoparticle catalysts. The suspensions were magnetically agitated for 30 minutes in the dark before being exposed to radiation to achieve adsorption equilibrium. The suspension were sampled periodically while they were subjected to irradiation and adsorption. 3 mL aliquots of reaction medium taken, and they were centrifuged for 15 min. A long, flexible needle-equipped syringe was used to carefully collect the supernatant, which was then centrifuged once more at the similar speed for the same amount of time. The catalyst's tiny particles were removed using a second centrifuge.

After the second centrifugation, the phenol's absorbed at its maximum wavelength of 269 nm was measured using a UV-visible spectrophotometer.

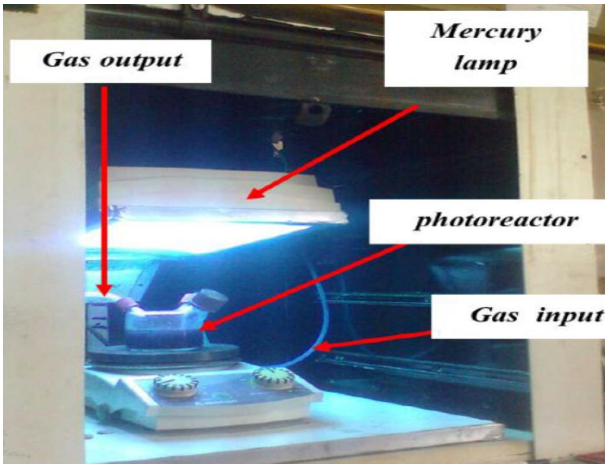

Figure 6: Experimental apparatus of photoreactions.

3. RESULTS AND DISCUSSION

3.1. Raman Spectroscopy

The lengthy maximum at 144 cm-1 (Eg) [177] is one of the key peak mostly in Raman data depicted in the pictures.

Although there are three groups that reference to rutile, the 515 cm-1 A1g maximum is the most intense for the rutile phase.[29-32]

All of the Raman spectrum for anatase phase in the TiO2 remain unchanged, with the exception of the composites' anatase Raman spectrum at 144 cm-1 and rutile one at 612 cm-1 being somewhat widened.

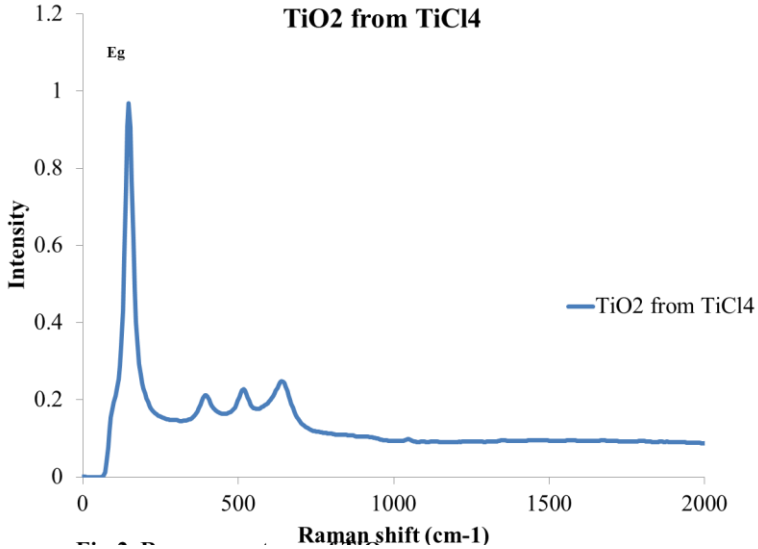

Figure 7: Raman spectrum of TiO2 sunthesis.

3.2. X-ray Diffraction Spectroscopy (XRD)

The average diameters of the crystallites (D) were determined use XRD data and Scherrer's equation in the following formula.[33-34]

$$D = \frac{k\lambda}{\beta cos\theta}$$

D is the typical crystalline size, k = 0.94 the fixed crystal lattice, X-ray wavelength of Cu K = 0.154 nm, is the peak's entire width calculated at half maximum intensity, and is the peak's Bragg's angle.

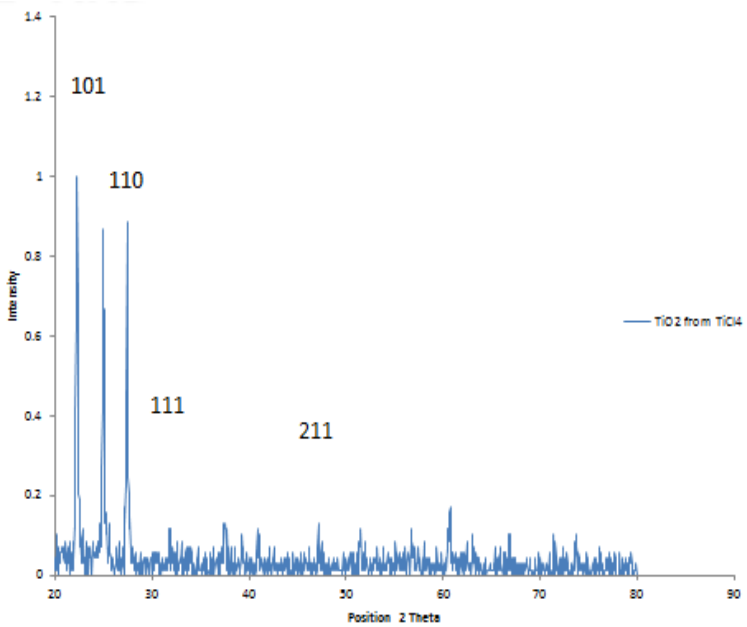

Figure 9: XRD of TiO2 synthesis.

Table 2: Average crystal size measured by XRD for samples.

Samples	Average crystal size /nm
P25	22.797
TiO2(TiCl4)	26.937

3.3. Scanning Electron Microscopy (SEM)

High vacuum was used to operate a SEM.The fundamental ideas are that an appropriate source produces an electron beam.To produce a narrow beam of electrons, a high voltage and passage sped the beam of electrons via a set of electromagnetic lenses and apertures. The thin beam of electrons was then utilized to scan the sample surface using scan coils.

Different electron image kinds exist.
The backscattering image and the secondary electron imaging are the two types.A high resolution image is primarily produced using the secondary electron imaging.[35-36] On a JEOL JSM-6700F apparatus, SEM measurements were performed to use a secondary electron detection (SE) at an applied potential of 2.0 kV.

Software known as Spip, or scanning prop image processor, was used to determine the average particle sizes.

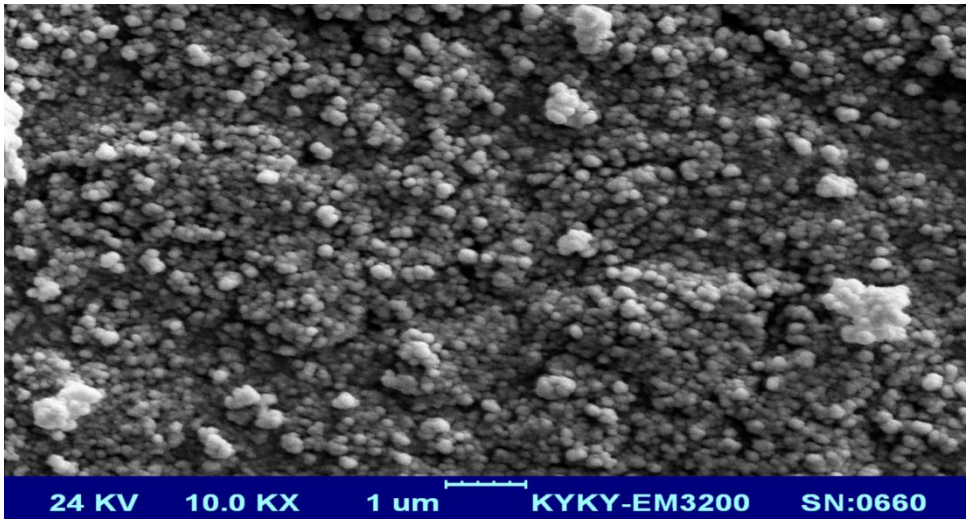

Figure 10: SEM of TiO2 synthesized.

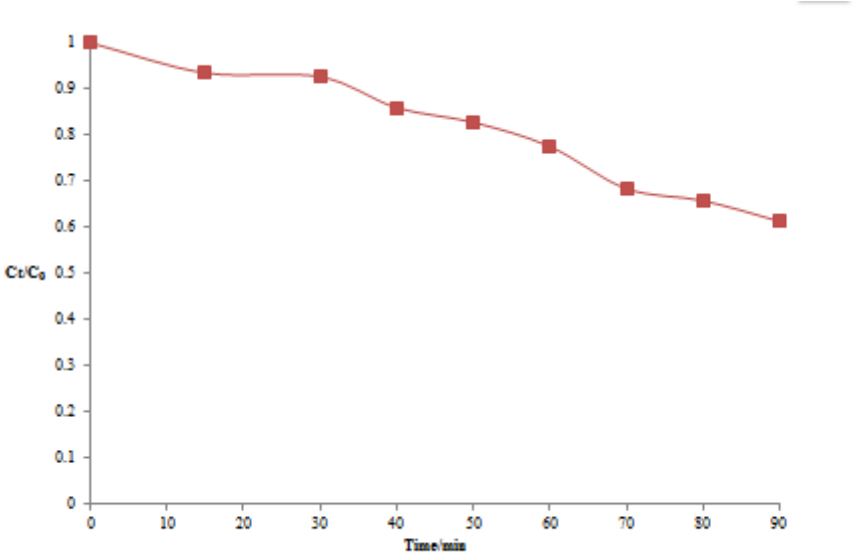

Figure 10: Photodegredation of phenol by TiO2 synthesized.

The Langmuir-Hinshelwood model can be used to describe the photocatalytic reactions occurring on TiO2 surfaces.

Following the adsorption equilibrium, the reaction rate can be written as: $ln\left(\frac{C_0}{C_t}\right) = kt$

Where k and t are the actual average speed constant and time, respectively, and Ct and Co are the component quantity at instances of time = t and t = 0, respectively.

The slope of k is obtained from a plotting of ln (Co/Ct) against t.

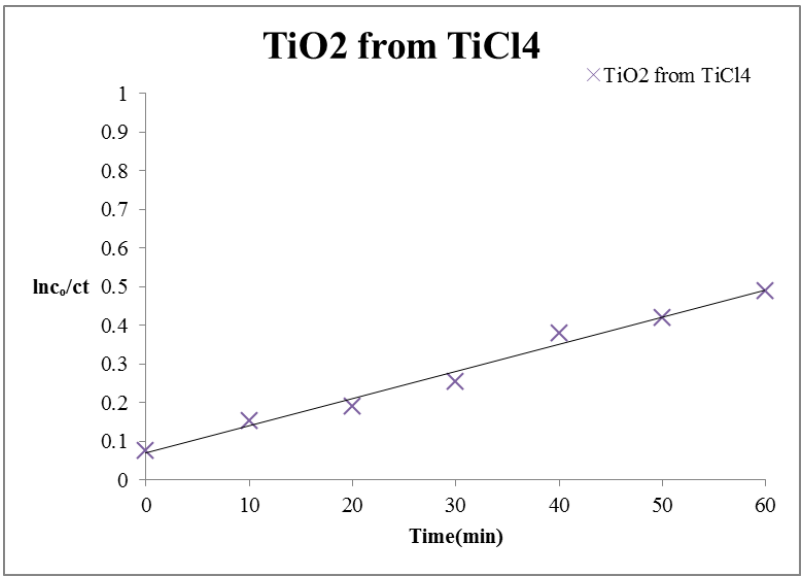

Figure 12: Photodegradation removal of phenol by TiO2 synthesized.

CONCLUSION

TiCl4 and absolute ethanol were used as additives in the effective synthesis of TiO2 nanoparticles utilizing sol gel.Anatase nanoparticle production was verified by XRD analysis. With an average particle size of roughly 26 nm across all samples, the maximum analysis of the XRD pattern revealed only the inclusion of two phases of pristine crystal structure, which may find use as UV shielding material. The findings showed that the top-notch TiO2 nanoparticles had an annealing temperature of 400°C and a volumetric precursor percentage of 50%.

Sol gel is a great way to create TiO2 nanoparticles, which are a semiconductor. Sol gel enhances the efficiency of photodegradation for pollutants by increasing surface area and decreasing particle size distribution, and it also produces nanoparticles, which results in high-throughput and economical processes.

The produced catalysts' TiO2 anatase characteristics were shown by XRD, SEM, and Raman analysis. According to adsorption and photocatalytic degradation of phenol by TiO2, the greatest elimination percentage was 77%.

REFERENCES

1. Majeed A. Shaheed And Falah H. Hussein , Synthesis and photocatalytic activity of TiO2 Nanoparticles, Journal of Babylon University/Pure and Applied Sciences, 2012; (22): College of Science/Babylon University Scientific Conference https://www.iasj.net/iasj/download/8dd7ce25c05e447b
2. Farah S Daabool, Falah H Hussein, Photocatalytic Degradation of Phenol Using TiO^ sub 2^/Active Carbon, Asian Journal of Chemistry, 2016; 282: 455. https://cdnx.uobabylon.edu.iq /research /repository1_publication 7711_18_2455.pdf.
3. Farah S. Daabool And Falah H. Hussein, Synthesis and Characterization of Active Carbon-Titanium Dioxide Composite, Asian Journal of Chemistry, 2019; 31(5): 1176-1180. https://asianpubs.org /index.php/ajchem/article /view/265/265
4. Keito Sano, Fazalurahman Kuttassery, Tetsuya Shimada, Tamao Ishida, Shinsuke Takagi, Bunsho Ohtani, Akira Yamakata, Tetsuo Honma, Hiroshi Tachibana, Haruo Inoue. Optically Transparent Colloidal Dispersion of Titania Nanoparticles Storable for Longer than One Year Prepared by Sol/Gel Progressive Hydrolysis/Condensation. ACS Applied Materials & Interfaces, 2020; 12(40): 44743-44753. https://doi.org/10.1021/acsami.0c12951
5. Mangey Ram Nagar, Shahnawaz, Rohit Ashok Kumar Yadav, Jin-Ting Lin, Jwo-Huei Jou. Nanocomposite Electron-Transport Layer Incorporated Highly Efficient OLED. ACS Applied Electronic Materials, 2020; 2(6): 1545-1553. https://doi.org/10.1021/acsaelm.0c001 66.
6. Yu-Hong Hu, Cong-Xue Liu, Jian-Cheng Wang, Xiu-Hui Ren, Xuan Kan, Yu-Bin Dong. TiO2@UiO-68-CIL: A Metal– Organic-Framework-Based Bifunctional Composite Catalyst for a One-Pot Sequential Asymmetric Morita–Baylis– Hillman Reaction. Inorganic Chemistry, 2019; 58(8): 4722-4730. https://doi.org/10.1021 /acs.inorgchem8b02132
7. Nathan A. Reed, Ramesh Raliya, Rui Tang, Baogang Xu, Matthew Mixdorf, Samuel Achilefu, Pratim Biswas. Electrospray Functionalization of Titanium Dioxide Nanoparticles with Transferrin for

Cerenkov Radiation Induced Cancer Therapy. ACS Applied Bio Materials, 2019; 2(3): 1141-1147. https://doi.org/10.1021 /acsabm.8b007 55

8. Felix Yu. Sharikov, Oleg A. Drozhzhin, Vasiliy D. Sumanov, Andrey N. Baranov, Artem M. Abakumov, and Evgeny V. Antipov . Exploring the Peculiarities of LiFePO4 Hydrothermal Synthesis Using In Situ Calvet Calorimetry. Crystal Growth & Design, 2018; 18(2): 879-882. https://doi.org /10.1021/acs.cgd.7b013 66.
9. Ronghua Li, Mickael Boudot, Cédric Boissière, David Grosso, and Marco Faustini. Suppressing Structural Colors of Photocatalytic Optical Coatings on Glass: The Critical Role of SiO2. ACS Applied Materials & Interfaces, 2017; 14102-4093(16): https://doi.org/10.1021/acsami.7b022 33.
10. Di Li, Xinyu Li, and Jinlong Gong. Catalytic Reforming of Oxygenates: State of the Art and Future Prospects. Chemical Reviews, 2016; 116(19): 11529-11653. https://doi.org/10.1021/acs.chemrev.6 b00099
11. Matteo Cargnello, Thomas R. Gordon, and Christopher B. Murray. Solution-Phase Synthesis of Titanium Dioxide Nanoparticles and Nanocrystals. Chemical Reviews, 2014; 114(19): 9319-9345. https://doi.org/10.1021 /cr500170p
12. Sedigheh Abedi and Ali Morsali. Ordered Mesoporous Metal–Organic Frameworks Incorporated with Amorphous TiO2 As Photocatalyst for Selective Aerobic Oxidation in Sunlight Irradiation. ACS Catalysis, 2014; 4(5): 1398-1403. https://doi.org/10.1021/cs500123d.
13. Xiangcun Li, Wenji Zheng, Gaohong He, Rui Zhao, and Dan Liu. Morphology Control of TiO2 Nanoparticle in Microemulsion and Its Photocatalytic Property. ACS Sustainable Chemistry & Engineering, 2014; 2(2): 288-295. https://doi.org/10.1021/sc400328u
14. Landry Biyoghe Bi Ndong, Murielle Primaelle Ibondou, Xiaogang Gu, Shuguang Lu, Zhaofu Qiu, Qian Sui, and Serge Maurice Mbadinga . Enhanced Photocatalytic Activity of TiO2 Nanosheets by Doping with Cu for Chlorinated Solvent Pollutants Degradation. Industrial & Engineering Chemistry Research, 2014; 53(4): 1368-1376. https://doi.org /10.1021/ie403405z
15. Chung-Yi Wu Yu-Shiu Lo Chien-Hou Wua. Thickness Dependent Photocatalytic Performance of Nanocrystalline TiO2 Thin Films, 2014; 85-109. https://doi.org/10.1021/bk-2014-1184.ch005
16. Jared T. Wabeke Hazim Al-Zubaidi Clara P. Adams Liyana A. Wajira Ariyadasa Setare Tahmasebi Nick Ali Bolandi Robert Y. Ofoli Sherine O. Obare . Synthesis of Nanoparticles for Biomass Conversion Processes, 2014; 219-246. https://doi.org/10.1021 /bk-2014-1186.ch012
17. Nitish Roy, Youngku Sohn, and Debabrata Pradhan. Synergy of Low-Energy {101} and High-Energy {001} TiO2 Crystal Facets for Enhanced Photocatalysis. ACS Nano, 2013; 7(3): 2532-2540. https://doi.org/10.1021/nn305877v
18. Sergey Ishchuk, Dereje Hailu Taffa, Ori Hazut, Niv Kaynan, and Roie Yerushalmi Transformation of Organic–Inorganic Hybrid Films Obtained by Molecular Layer Deposition to Photocatalytic Layers with Enhanced Activity. ACS Nano, 2012; 6(8): 7263-7269.https://doi.org/10.1021/nn302370y
19. Jian-Chun Wu, Jianwei Zheng, Ping Wu, and Rong Xu. Study of Native Defects and Transition-Metal (Mn, Fe, Co, and Ni) Doping in a Zinc-Blende CdS Photocatalyst by DFT and Hybrid DFT Calculations. The Journal of Physical Chemistry C., 2011; 115(13): 5682https://doi.org/10.1021 /jp109567c
20. Nichola M. Kinsinger, Ashley Wong, Dongsheng Li, Fabian Villalobos, and David Kisailus. Nucleation and Crystal Growth of Nanocrystalline Anatase and Rutile Phase TiO2 from a Water-Soluble Precursor. Crystal Growth & Design, 2010; 10(12): 5254-5261.https://doi.org/10.1021/cg101105t
21. Xiaobo Chen, Shaohua Shen, Liejin Guo, and Samuel S. Mao. Semiconductor-based Photocatalytic Hydrogen Generation. Chemical Reviews, 2010; https://doi.org/10.1021/cr1001645.
22. Ujwal Shreenag Meda, Khushi Vora, Yash Athreya, Ujwal Arun Mandi. Titanium dioxide based heterogeneous and heterojunction photocatalysts for pollution control applications in the construction industry. Process Safety and Environmental Protection, 2022; 787-771 https://doi.org/10.1016 /j.psep.2022.03066
23. Muhammad Bilal Tahir, Sohail Farman, Muhammad Sagir. Advances in Photocatalytic Materials for Waste Water Treatment Applications, 2022; 759-767. https://doi.org/10.1016/B978-0-12-815732-9.00032-2
24. Yunhong Shi, Awatef Abidi, Yacine Khetib, Long Zhang, Mohsen Sharifpur,Goshtasp Cheraghian. The computational study of nanoparticles shape effects on thermal behavior of H2O-Fe nanofluid: A molecular dynamics approach. Journal of Molecular Liquids, 2022; 346: 117093. https://doi.org/10.1016 /j.molliq.2021. 117093
25. Andrey A. Rempel, Albina A. Valeeva, Alexander S. Vokhmintsev, Ilya A. Weinstein. Titanium dioxide nanotubes: synthesis, structure, properties and applications. Russian Chemical Reviews, 2021; 90(11): 1397-1414. https://doi.org/10.1070/RCR 4991.
26. Golnoush Zamiri, Samira Bagheri, Arman Amani Babadi, Seyedehmaryam Moosavi, M.S. Naghavi. The impact of immerssion time and thickness of TiO2 photoanode on power conversion efficiency of dye-sensitised solar cells using graphene quantum dots as photosensitiser. Optical Materials, 2021; 111720: 122. https://doi.org/10.1016/j.optmat.2021. 111720.
27. Yunhong Shi, Seyedmahmoodreza allahyari, S. Mohammad Sajadi, Mashhour A. Alazwari, Payam Firouzi, Nidal H. Abu-Hamdeh, Ferial Ghaemi,

Dumitru Baleanu, Arash Karimipour. The Molecular dynamics study of atomic Management and thermal behavior of Al-Water Nanofluid: A two phase unsteady simulation. Journal of Molecular Liquids, 2021; 340: 117286. https://doi.org/10.1016 /j.molliq.2021. 117286

28. Büşra BULUT, Şeyma duman. Effects of calcination temperature on hydrothermally synthesized titanium dioxide submicron powders. Konya Journal of Engineering Sciences, 2021; 703-712. https://doi.org/10.36306/konjes.91506 2
29. Damiano Cani, Jan C. van der Waal, Paolo P. Pescarmona. Highly-accessible, doped TiO2 nanoparticles embedded at the surface of SiO2 as photocatalysts for the degradation of pollutants under visible and UV radiation. Applied Catalysis A: General, 2021; 621: 118179. https://doi.org/10.1016 /j.apcata.2021. 118179
30. Katarzyna Siuzdak, Łukasz Haryński, Jakub Wawrzyniak, Katarzyna Grochowska. Review on robust laser light interaction with titania – Patterning, crystallisation and ablation processes. Progress in Solid State Chemistry, 2021; 62: 100297. https://doi.org/10.1016/j.progsolidstch em.2020.100297
31. M. Davide Cappelluti, Emina Hadzifejzovic, John S. Foord, Duncan H. Gregory. Flash microwave-assisted solvothermal (FMS) synthesis of photoactive anatase sub-microspheres with hierarchical porosity. RSC Advances, 2020; 10(61): 37233-37245. https://doi.org/10.1039/D0RA05796G
32. Eka Cahya Prima, Harbi Setyo Nugroho, Nugraha, Gema Refantero, Camelia Panatarani, Brian Yuliarto. Performance of the dye-sensitized quasi-solid state solar cell with combined anthocyanin-ruthenium photosensitizer. RSC Advances, 2020; 10(60): 36873-36886. https://doi.org/10.1039 /D0RA06550A
33. Sijia Sun, Hao Ding, Jie Wang, Wei Li, Qiang Hao. Preparation of a microsphere SiO2/TiO2 composite pigment: The mechanism of improving pigment properties by SiO2. Ceramics International, 2020; 46(14): 22944-22953. https://doi.org/10.1016 /j.ceramint.202 0.06.068
34. Yoongook Park, Jun Hyup Lee. Wide viewing optically clear adhesives using PMMA/TiO 2 core-shell micro/nanoparticles. Molecular Crystals and Liquid Crystals, 2020; 705(1): 135-140. https://doi.org/10.1080/15421406.202 0.1743430
35. Daniel D. Lane, Kvar C. L. Black, Ramesh Raliya, Nathan Reed, Nalinikanth Kotagiri, Rebecca Gilson, Rui Tang, Pratim Biswas, Samuel Achilefu. Effects of core titanium crystal dimension and crystal phase on ROS generation and tumour accumulation of transferrin coated titanium dioxide nanoaggregates. RSC Advances, 2020; 10(40). .https://doi.org /10.1039/D0RA01878C.